

## Microphotoluminescence study of individual suspended ZnO nanowires

Min Gao,<sup>1,a)</sup> Wenliang Li,<sup>1</sup> Yang Liu,<sup>1</sup> Quan Li,<sup>2</sup> Qing Chen,<sup>1</sup> and Lian-Mao Peng<sup>1</sup>

<sup>1</sup>Key Laboratory for the Physics and Chemistry of Nanodevices and Department of Electronics, Peking University, Beijing 100871, People's Republic of China

<sup>2</sup>Department of Physics, The Chinese University of Hong Kong, Shatin, New Territory, Hong Kong

(Received 9 January 2008; accepted 25 February 2008; published online 20 March 2008)

We report microphotoluminescence measurements on individually suspended ZnO nanowires attached to nanometer-sized metal tips. This procedure avoids the possible influence of the substrate and enables comprehensive optical, electrical, chemical, and morphological characterizations to be carried on the same individual nanowire. Based on the ZnO nanowires examined, we found that the near band edge emission redshifted with the increasing intensity of the defect-related green emission. The comprehensive characterizations of *in situ* heated ZnO nanowires suggested a correlation between the defect green emission and the oxygen deficiency, which also affect the carrier density, and thus, the nanowire's transport property. © 2008 American Institute of Physics. [DOI: 10.1063/1.2898168]

The recent developments on optoelectronic nanodevices require not only nanoscale manipulation and processing of semiconducting nanostructures but also characterization of optical, electrical, and structural properties with resolution and sensitivity of individual nanostructures.<sup>1-3</sup> Correspondingly, great efforts have been made to develop photoluminescence (PL), one of the most important characterization techniques of semiconductor properties, into a local technique.<sup>4</sup> PL from individual nanostructures has been realized in, e.g., quantum dots, carbon nanotubes, and nanowires.<sup>3-6</sup> In such studies, the nanostructures are usually embedded (quantum dots) in or dispersed on substrates.<sup>3-6</sup> Due to the large surface-volume ratios of nanostructures, the electronic structure and thus the luminescence property are expected to be strongly dependent on the environment, e.g., surface absorption and substrate.<sup>7</sup>

In this paper, we report a versatile procedure for carrying out micro-PL measurements on suspended individual semiconductor nanowires. This procedure utilizes nanoprobe manipulation inside a scanning electron microscope (SEM), enabling comprehensive optical, electrical, and microstructure characterization of the same nanowire. We show that such comprehensive characterization yields insights on the behavior and nature of the UV near band edge (NBE) emission and defect-related green emission of ZnO nanowires, which have been highly focused topics, but still under debate.<sup>8-12</sup>

The micro-PL system used in this study was built based on an Olympus optical microscope. The sample is excited by a 325 nm wavelength laser beam focused into a  $<1 \mu\text{m}$  spot through a long focal length UV objective lens. The ZnO nanowires used in this study were synthesized by thermal evaporation of pure ZnO powder (99.99%) at 1200 °C. The base pressure inside the alumina tube furnace was  $2 \times 10^{-2}$  Torr. The source material was loaded at the center of the tube and the products were collected at the downstream of the tube. We use a FEI XL30 SFEG SEM equipped with 4 Kleindiek nanoprobe manipulators and an EDAX EDS spectrometer to carry out microstructure and composition characterization, nanoscale manipulation, and *in situ*

transport measurements. A Keithley 4200 semiconductor characterization system was used for the *in situ* *I-V* measurements. For the *in situ* heating experiment, stable contacts were first obtained using the Joule heating effect and e-beam exposure described in previous work.<sup>13</sup>

The SEM image in Fig. 1(a) illustrates the preparation of an individual suspended nanowire using nanoprobe manipulation. We drive a nanometer-sized tungsten (W) tip to make contact with the selected as-grown ZnO nanowire loosely bounded to the end of a flattened Pt wire. The contact area is then illuminated by the electron beam so that amorphous carbon can be deposited locally to "glue" the W tip and the end of the nanowire together.<sup>14</sup> By moving the W tip away from the Pt wire, an individual suspended nanowire is ob-

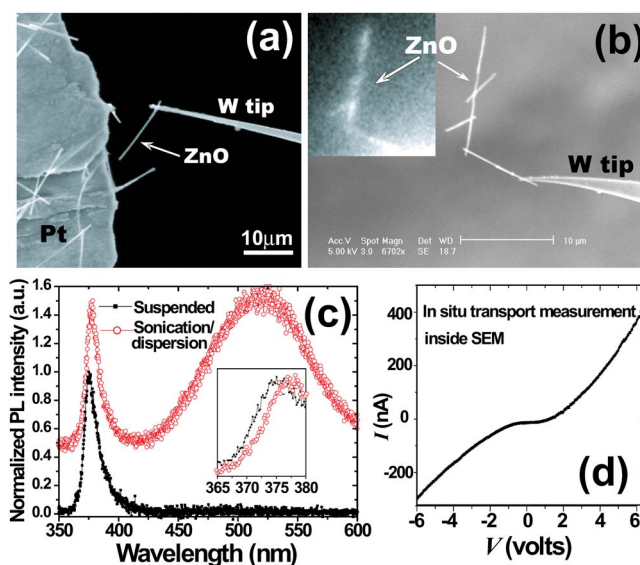


FIG. 1. (Color online) (a) SEM image illustrating the preparation of suspended individual nanowires by nanoprobe manipulation inside SEM. (b) SEM and optical (inset) images showing the same chain of ZnO nanowires glued to a W tip. (c) Micro-PL spectra of an individual suspended as-grown ZnO nanowire and an individual ZnO nanowire processed by sonication/dispersion procedure. Both nanowires have regular cross section and similar diameters ( $\sim 50$  nm). The inset compares the onset parts of the NBE emission of the two nanowires. (d) A typical two-terminal *I-V* curve of individual suspended ZnO nanowires.

<sup>a)</sup> Author to whom correspondence should be addressed. Electronic mail: mingao@pku.edu.cn.

tained and can then be taken out of the SEM with the metal tips and the nanomanipulator for micro-PL measurements. The incorporation of the nanomanipulator with the micro-PL measurement enables convenient identification of the nanowire position using the SEM images as reference, since the orientation of the nanowire can be maintained. Figure 1(b) displays such an example.

Figure 1(c) shows a typical PL spectrum of suspended individual ZnO nanowires. Similar to some of the previous reports,<sup>9</sup> the PL spectra of the as-grown nanowires consist of a UV NBE emission peak and a broad defect-related deep level emission at  $\sim 520$  nm. All the spectra shown in this paper were obtained under very low excitation power ( $\sim 5$  W/cm<sup>2</sup>) which tends to maximize the visibility of the defect emission.<sup>15,16</sup> Employment of the suspended individual nanowires attached to metal tips also provides a technique compatible with established electrical measurement using the *in situ* nanoprobe technique inside SEM.<sup>13</sup> For example, *I-V* curve [Fig. 1(d)] can be measured before the nanowire is removed from the Pt wire with the W tip and flattened Pt wire as electrodes. Our results show that the ZnO nanowires usually exhibit stable contact with Pt wires probably due to the relatively large contact areas and the cleanliness of the Pt surface. Thus, optical (PL), microstructural (SEM), and electrical (nanoprobe technique) characterization can be carried out on the same nanowire.

Compared to the usual micro-PL measurements of individual nanowires, in which the nanowires are separately distributed on flat substrates, the procedure described here can effectively avoid the complex influences of the substrates and the often necessary sonication process in solutions. Indeed, we have observed that such sonication process may cause dramatically decreased UV emission and increased defect emission. Figure 1(c) compares PL spectra of a sonication processed ZnO nanowire lying on SiO<sub>2</sub>/Si substrate and an individual suspended as-grown ZnO nanowire, showing a much stronger green emission and a redshift of the NBE emission in the sonication processed ZnO nanowire, likely being resulted from the surface change after solution sonication.

We now present our results on the correlations of the room temperature luminescence properties with the ZnO nanowire diameter. SEM results showed that most as-grown nanowires used in this study possessed circular cross section and smooth surface (corresponding to straight boundary and uniform contrast in the side view), in which green emission was observed to be normally one to two orders lower than the UV emission. On the other hand, a small percentage (<5%) of nanowires with irregular cross section and rough surface (slightly wavy boundary and varying contrast in the side view) usually exhibited much stronger “green” emission intensities and weakened UV emission (Fig. 2). The UV peak position from different individual ZnO nanowires was observed to vary slightly between 375 and 380 nm, corresponding to  $\sim 43.5$  meV difference in energy. We have carried out micro-PL measurements on individual suspended nanowires with a wide diameter distribution (30–150 nm). Unlike those studies showing anomalous blueshift in UV emission with decreasing nanowire diameter in the similar diameter range,<sup>11,12</sup> our results showed that the UV emission peak energy had little dependence on the diameter, but exhibited a strong tendency to redshift with the increase of the green defect emission, indicating defect induced modification of

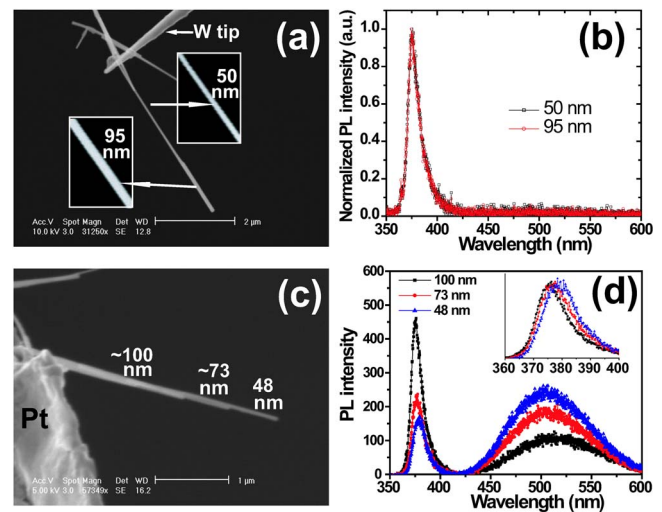


FIG. 2. (Color online) Side-view SEM images of regular (a) and irregular (c) shape individual suspended as-grown ZnO nanowires with changing diameters and micro-PL spectra [(b) and (d)] along their lengths. The insets in (a) show straight boundaries and uniform contrast of the two sections. The inset in (d) shows the redshift of the UV emission with decreasing diameter for the irregular shaped nanowire.

the electronic structure. The above conclusions are based on comparison not only among different nanowires but also on the same individual nanowires with varying diameters. To make a brief demonstration, we show PL results from two suspended as-grown ZnO nanowires with changing diameters (see Fig. 2). For the nanowire with regular shape shown in Fig. 2(a), only slight difference in UV to visible emission ratios was observed for the two parts with different diameters [Fig. 2(b)]. Correspondingly, UV emission peaks have almost the same position at 375.2 nm [Fig. 2(b)]. On the other hand, for the nanowire with irregular shape and rougher surface [Fig. 2(c)], with the decrease of the diameter, dramatically increased green emission and decreased UV emission can be observed [Fig. 2(d)], which was accompanied by the redshift of the UV emission peak energy from 375.6 to 379 nm.

The correlation between the UV emission redshift and the green emission was also observed in the *in situ* heating experiment of individual suspended nanowire inside SEM. For a suspended ZnO nanowire, the generated heat due to electrical current may not be effectively transferred from the center of the nanowire, so a temperature gradient can be expected from the center of the nanowire to the electrodes. Figure 3(a) shows a suspended nanowire of 150 nm in diameter and  $>20$   $\mu$ m in length. The accumulated heating at a current of  $\sim 3$   $\mu$ A resulted in an eventual “burnt-out” near the center of the nanowires [Fig. 3(b)]. X-ray energy dispersive spectroscopy (EDS) and electrical transport measurements were performed during the *in situ* heating experiment inside SEM. The EDS spectra [Fig. 3(c)] taken from the same position before and after heating, indicate a remarkable oxygen loss ( $<5\% \pm 1\%$  in the areas close to the burnt-out point) during the *in situ* annealing process. The transport measurements [Fig. 3(d)] shows that with the increasing annealing time, the conductance first increases abruptly and then increases slowly, followed by a decrease even before the observable change in the nanowire shape. This is probably corresponding to the increase of carrier density and decrease of carrier mobility during the *in situ* annealing process in vacuum.

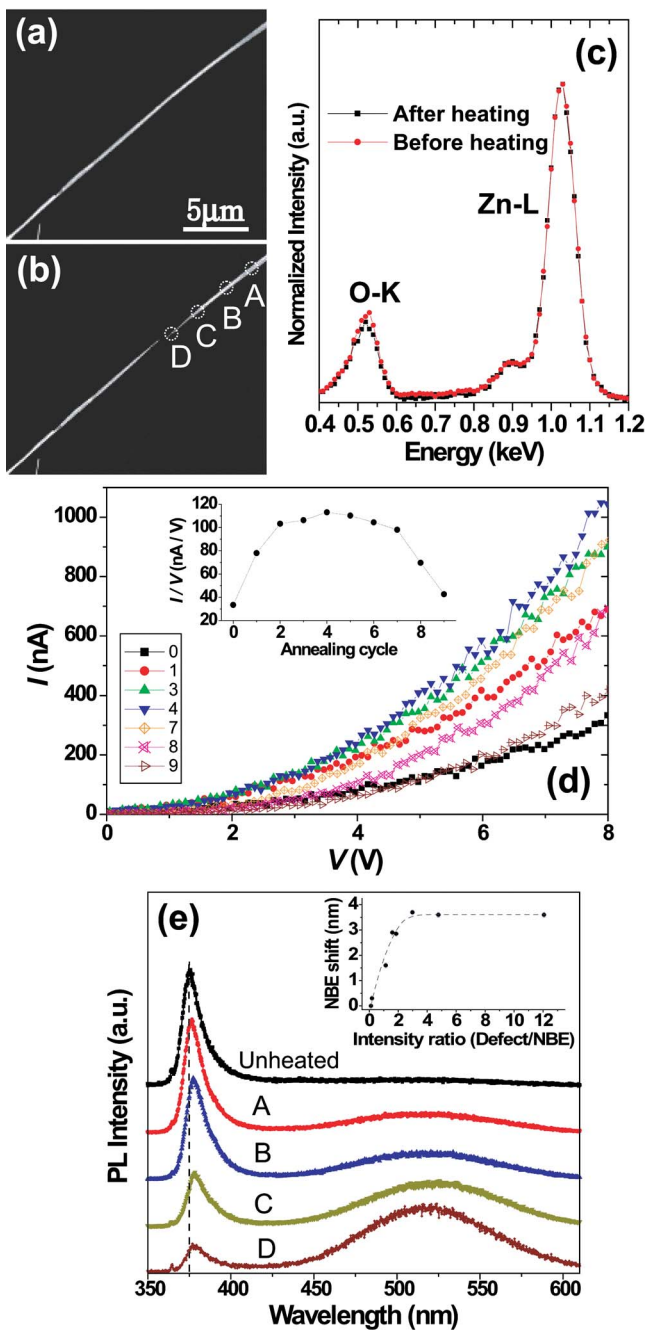


FIG. 3. (Color online) [(a) and (b)] SEM images showing a suspended ZnO nanowire before (a) and after (b) *in situ* burnt-out by electrical current. (c) EDS spectra from position close to the burnt-out spot before and after the *in situ* heating. (d) *I-V* curves during the interval of *in situ* heating. The numbers indicate the cycle of the heating. The inset shows the electrical conductance at 7 V. Before measuring each *I-V* curve, the heating process was paused for 20 min to let the nanowire cool down. Electron beam was blocked during all the transport measurements. (e) Micro-PL spectra from the unheated nanowire and the different positions [marked in Fig. 3(b)] after the burnt-out. The inset plots the redshift of the NBE peak vs the integrated intensity ratio between the deep level emission and NBE emission. The dashed line is used as a guide for the eye.

Figure 3(e) shows micro-PL spectra of the unheated nanowire and along different locations of the nanowire after the burnt-out, showing a dramatically increased green emission and a noticeable UV emission redshift with the temperature increase. This tendency has been confirmed to be independent of the burnt-out tip shape and diameter which can be varied by controlling the electrical current and the positions of the two electrodes. The correlation of PL, electrical trans-

port, and EDS measurements indicates that the UV emission redshift, green emission, and carrier density are closely related to oxygen deficiency. Recent calculation and experimental results indicate that Zn interstitials, acting as shallow donor in ZnO, have high formation energy and are not likely to form.<sup>17,18</sup> Therefore, the enhanced green emission intensity at higher annealing temperature is attributed to the population rising of the O vacancies, which has been shown to be a deep donor.<sup>19</sup> The co-occurrence of the redshift of the band edge emission and the increasing green emission must be attributed to other reasons, as the O vacancy does not serve as shallow donors in ZnO and Zn interstitials are not likely to form. Our results may support native defect complexes<sup>20</sup> and/or hydrogen at oxygen sites<sup>18,19</sup> serving as stable and effective shallow donor, although we cannot identify the donor conclusively. The hydrogen can come from the diffusion within the ZnO nanowire, the residual gas in the vacuum and ZnO nanowire surface absorption.

In conclusion, we have developed a general procedure which allows optical, electrical, and microstructural characterization of individual suspended quasi-one-dimensional nanostructures attached to nanometer-sized W tips. Our microphotoluminescence results from individual ZnO nanowires grown by thermal evaporation showed that a strong green emission can cause redshift of the NBE emission. Correlation of PL, electrical transport, and EDS measurements on *in situ* annealed ZnO nanowires proved that the green emission and the carrier behaviors are related to oxygen deficiency.

This work was supported by the Ministry of Science and Technology (Grant Nos. 2006CB932401 and 2006AA03Z350) and National Science Foundation (Grant Nos. 50702002, 10434010, 90606026) of China.

- <sup>1</sup>R. Agarwal and C. M. Lieber, *Appl. Phys. A: Mater. Sci. Process.* **85**, 209 (2006).
- <sup>2</sup>Y. Li, F. Qian, J. Xiang, and C. M. Lieber, *Mater. Today* **9**, 18 (2006).
- <sup>3</sup>M. Freitag, J. Chen, J. Tersoff, J. C. Tsang, Q. Fu, J. Liu, and P. Avouris, *Phys. Rev. Lett.* **93**, 076803 (2004).
- <sup>4</sup>H. Kalt, *Lect. Notes Phys.* **658**, 51 (2005).
- <sup>5</sup>J. F. Wang, M. S. Gudiksen, X. F. Duan, Y. Cui, and C. M. Lieber, *Science* **293**, 1455 (2001).
- <sup>6</sup>L. Wischmeier, T. Voss, S. Börner, and W. Schade, *Appl. Phys. A: Mater. Sci. Process.* **84**, 111 (2006).
- <sup>7</sup>J. Lefebvre, Y. Homma, and P. Finnie, *Phys. Rev. Lett.* **90**, 217401 (2003).
- <sup>8</sup>K. Vanheusden, W. L. Warren, C. H. Seager, D. R. Tallant, J. A. Voigt, and B. E. Gnade, *J. Appl. Phys.* **79**, 7983 (1996).
- <sup>9</sup>A. B. Djurišić and Y. H. Leung, *Small* **2**, 944 (2006).
- <sup>10</sup>A. B. Djurišić, Y. H. Leung, K. H. Tam, Y. F. Hsu, L. Ding, W. K. Ge, Y. C. Zhong, K. S. Wong, W. K. Chan, H. L. Tam, K. W. Cheah, W. M. Kwok, and D. L. Phillips, *Nanotechnology* **18**, 095702 (2007).
- <sup>11</sup>C. W. Chen, K. H. Chen, C. H. Shen, A. Ganguly, L. C. Chen, J. J. Wu, H. I. Wen, and W. F. Pong, *Appl. Phys. Lett.* **88**, 241905 (2006).
- <sup>12</sup>P. C. Chang, C. J. Cheien, D. Stichtenoth, C. Ronning, and J. G. Lu, *Appl. Phys. Lett.* **90**, 113101 (2007).
- <sup>13</sup>Q. Chen, S. Wang, and L.-M. Peng, *Nanotechnology* **17**, 1087 (2006).
- <sup>14</sup>M. S. Wang, J. Y. Wang, Q. Chen, and L.-M. Peng, *Adv. Funct. Mater.* **15**, 1825 (2005).
- <sup>15</sup>B. Guo, Z. R. Qiu, and K. S. Wong, *Appl. Phys. Lett.* **82**, 2290 (2003).
- <sup>16</sup>W. S. Shi, B. Cheng, L. Zhang, and E. T. Samulski, *J. Appl. Phys.* **98**, 083502 (2005).
- <sup>17</sup>A. Janotti and C. G. Van de Walle, *J. Cryst. Growth* **287**, 58 (2006).
- <sup>18</sup>A. Janotti and C. G. Van de Walle, *Appl. Phys. Lett.* **87**, 122102 (2005).
- <sup>19</sup>F. A. Selim, M. H. Weber, D. Solodovnikov, and K. G. Lynn, *Phys. Rev. Lett.* **99**, 085502 (2007).
- <sup>20</sup>D. C. Look, G. C. Farlow, S. Limpijumnong, S. B. Zhang, and K. Nordlund, *Phys. Rev. Lett.* **95**, 225502 (2005).